This document is the Accepted Manuscript version of a Published Work that appeared in final form in [The FEBS Journal], Copyright © 2016 The Authors. To access the final published work see [**https://doi.org/10.1111/febs.13901**]

**REGULAR PAPER**

**TITLE:**

# Dexamethasone improves redox state in Ataxia Telangiectasia cells by promoting NRF2-mediated antioxidant response

**AUTHORS:**

Sara Biagiotti[1], Michele Menotta[1], Sara Orazi[1], Chiara Spapperi[1], Serena Brundu[1], Alessandra Fraternale[1], Marzia Bianchi[1], Luigia Rossi[1], Luciana Chessa[2] and Mauro Magnani[1]

**AFFILIATIONS:**

[1]Department of Biomolecular Sciences, University of Urbino "Carlo Bo", 61029 Urbino (PU), Italy
[2]Department of Clinical and Molecular Medicine, University "La Sapienza", 00198 Roma, Italy

**CORRESPONDING AUTHOR:**

Dr. Sara Biagiotti, Ph.D.
Department of Biomolecular Sciences
University of Urbino "Carlo Bo"
Via Saffi 2, 61029 Urbino (PU), ITALY
Tel.: +39 0722 305232
Fax: +39 0722 305324
e-mail: sara.biagiotti@uniurb.it.

**RUNNING TITLE**

Effect of Dexa on oxidative stress in A-T cells

**ABBREVIATIONS**

Ataxia Telangiectasia, A-T
Dexamethasone, Dexa
Dimethylsulfoxide, DMSO
Lymphoblastoid Cell Lines, LCLs
Nicotinamide Adenine Dinucleotide Phosphate, NADPH
Nuclear Factor (erythroid-derived 2)-like 2, NRF2
Pentose Phosphate Pathway, PPP
Pyruvate Dehydrogenase Kinase, PDK
Reduced Glutathione, GSH

**KEYWORDS**

Ataxia Telangiectasia; Glucocorticoids; Oxidative stress; Nuclear factor 2; Molecular cell biology.

**CONFLICTS OF INTEREST**

The authors declare that they have no conflicts of interest with the contents of this article.

## ABSTRACT

Ataxia Telangiectasia (A-T) is a rare incurable neurodegenerative disease caused by biallelic mutations in the ATM gene. The lack of a functional ATM kinase leads to a pleiotropic phenotype, and oxidative stress is thought to have a crucial role in the complex physiopathology. Recently, steroids have been shown to reduce the neurological symptoms of the disease, but the molecular mechanism of this effect is largely unknown. We demonstrated that dexamethasone treatment of A-T lymphoblastoid cells increases the content of two of the most abundant antioxidants, GSH and NADPH, by up to 30%. Dexamethasone promoted the nuclear accumulation of the transcription factor NRF2 to drive expression of antioxidant pathways involved in glutathione synthesis and NADPH production. The latter effect was via G6PD activation, as confirmed by increased enzyme activity and enhancement of the pentose phosphate pathway rate. This evidence indicates that glucocorticoids are able to potentiate antioxidant defenses to counteract oxidative stress in Ataxia Telangiectasia, and reveal an unexpected role for dexamethasone in redox homeostasis and cellular antioxidant activity.


## INTRODUCTION

Ataxia Telangiectasia (A-T) is a neurodegenerative disease with autosomal recessive inheritance and, despite being monogenic, is characterized by a very pleiotropic phenotype. In addition to the well-known role of ATM in the DNA damage response, the phosphorylation landscape and functions of this versatile protein are also the focus of growing interest [1-6]. The lack of kinase activity leads to the impairment of a very large network of signalling pathways, including regulation of the cellular redox homeostasis and metabolic pathways [7-14]. Metabolic defects are thought to play a crucial role in the complex physiopathology [15-18] and the resulting altered metabolism can be a source of oxidative stress [19].

In recent years, oxidative stress has been profusely singled out. Indeed, the link between oxidative stress and A-T is well established, but mainly relies on studies performed in *in vitro* or in animal models [20-25]. Those studies suggested that oxidative stress may actively contribute to the oddest degenerations in A-T cells, even before ATM functions in redox homeostasis were known.

Despite the poor evidence collected in patients, dietary antioxidants have been largely accepted as supportive therapies in people suffering from Ataxia Telangiectasia [26-28]. Although the lifespan of patients with A-T has been prolonged over the years, no established therapy is currently available. Recently, the glucocorticoid analogues, Betamethasone and Dexamethasone, have been successfully proposed as a novel treatment for A-T patients [29-36], but their mechanism of action is still under investigation [37;38]. We have previously reported that Dexamethasone can partially rescue ATM deficiency by promoting a shortened protein variant [39]. In addition, we have identified the meaningful pathways required for the drug action [40].

In this investigation, we attempted to delineate new links between Ataxia Telangiectasia, oxidative stress and glucocorticoid action. Our results provide evidence that Dexametasone (Dexa) treatment could improve the antioxidant capacity of A-T cells by enriching the pool of antioxidant molecules. In addition, we propose new molecular mechanisms for this drug, which are mechanistically related to the intrinsic pathogenic mechanisms of Ataxia Telangiectasia.

## RESULTS

Effect of Dexa on antioxidant molecules

Glutathione is the most abundant scavenger molecule within cells; thus, we started by measuring reduced glutathione (GSH). Experiments were performed on lymphoblastoid cells lines (LCLs) derived from three A-T patients (AT50RM, AT28RM, AT129RM,**TABLE 1**) and compared to those derived from a healthy donor (WT). Suitable samples were extracted from LCLs with or without Dexa administration. In agreement with other studies [41-45], we found that basal levels of GSH do not differ significantly in A-T cells compared to wild type (WT) cells (**FIGURE 1A**). Even more interestingly, we observed a significant increase in GSH content after 24 hours of exposure to Dexa in both wild type and mutated cells (ranging from 20 to 30%). GSH content, assayed again after 48 hours of Dexa exposition, did not increase further. It is noteworthy that A-T cells treated with Dexa displayed GSH levels that were even higher than basal WT cells (Wilcoxon signed rank test WT versus each A-T cell line $p<0.05$). To our knowledge, this is the first time that it has been shown that glucocorticoids are capable of augmenting the GSH pool in A-T cells.

We subsequently assessed whether the significant increase observed in GSH content after Dexamethasone administration could be due to redox-cycling of glutathione. Indeed, glutathione exists in both reduced and oxidized (GSSG) states but, under normal conditions, GSSG accounts for only 5-10% of total glutathione. We showed that Dexa is able to significantly increase both reduced and total glutathione in A-T cells (**FIGURE 1B**). On the contrary, GSSG content was unaffected. This is consistent with the hypothesis that Dexa enriches the total glutathione pool to possibly counteract oxidative stress.

To support our hypothesis, we measured reduced glutathione upon induction of an oxidative stress. Unfortunately, lymphoblastoid cells proved to be too sensitive to hydrogen peroxide, which was found to be associated with a reduced survival and did not allow us to reliably assess GSH content under stressful conditions. Thus, we performed the same investigations in primary fibroblasts from A-T patients. Specifically, stress was triggered by 0, 25 and 50 µM hydrogen peroxide. As shown in **FIGURE 1C**, Dexa was also able to increase GSH levels in fibroblasts. Moreover, the drug was able to protect cells preventing GSH depletion. In fact, comparing data from control and treated fibroblasts, GSH contents were found to be significantly higher even when cells were subjected to hydrogen peroxide.

GSH/GSSG is the major redox couple that determines the antioxidant capacity of cells, but its value can be affected by other redox pairs, especially the NADPH/$NADP^+$ ratio. We therefore measured NADPH and $NADP^+$ in WT and A-T lymphoblastoid cell lines with or without Dexa. We observed that Dexamethasone raised NADPH concentration both in normal and mutant LCLs (**FIGURE 2A**). $NADP^+$ concentrations were also measured to estimate the NADPH/$NADP^+$ ratio and the obtained values are shown in **FIGURE 2B**. All LCLs showed an increased ratio after drug treatment compared with the respective untreated samples, which is consistent with an increased reducing power. In fact, comparison of $NADP^+$ levels among each cell line does not find out any statistical difference neither between basal WT and AT nor between treated ones.

Given its synergic effect on both glutathione and NADPH, it can be argued that Dexa enhances cellular antioxidant capacity. Since oxidative stress is the result of an imbalance between antioxidant and pro-oxidant species, we sought to complete the picture by assessing reactive oxygen species content. ROS were evaluated by dichlorofluorescein assay in WT and A-T lymphoblastoid cells treated with Dexa or untreated. Basal ROS levels were undetectable in WT and AT50RM, while AT28RM and AT129RM showed detectable ROS levels even at rest. Accordingly with the observed increased antioxidant capacity, Dexa also reduces ROS production (**FIGURE 3**). This is in agreement with the observations of Russo et al. [34], who documented a remarkable reduction in ROS levels in a single patient studied at different time-points of betamethasone therapy.

Effect of Dexa on the antioxidant response

After showing that Dexa was able to strengthen the cellular antioxidant defences increasing the cell's redox capacity, we turned our attention to the underlying mechanisms of action of the drug.

A set of pathways can control antioxidant molecules within cells. All these pathways belong to a complex network of molecular signals that together constitute the antioxidant response. These molecular pathways need to be finely controlled and regulation mainly occurs via transactivation of the respective antioxidant genes.

Among the various branches, we focused on GSH metabolism and NADPH production. To this end, a quantitative PCR array was set up to address when and whether Dexa could enhance antioxidant gene expression. Selected target genes are listed in **TABLE 2**. A preliminary time-course analysis conducted in AT129RM revealed the upregulation of most genes after a 24-hour treatment. Results are summarized in **FIGURE 4A**. Unfortunately, targets belonging to GSH utilization were undetectable.

After having tested the effect of Dexa on the whole targets, we assayed the entire panel of genes in the remaining A-T cells. The same assays were performed on WT genes as a control. As shown in **FIGURE 4B,** overexpression of the whole genes of GSH synthesis was validated, as it was the most significant effect on glutamylcysteine ligase catalytic subunit (GCLC). Both the catalytic and modifier subunit of glutamyl-cysteine ligase (GCL) were found to be significantly overexpressed in all LCLs, while glutathione synthetase (GSS) was upregulated in all cells but significantly so in two out of three. It is notable that Dexa was able to induce those genes in A-T cells but not in WT cells. Moreover, glutathione reductase (GSR) was found to be slightly upregulated in A-T cells but not in WT cells. Regarding the last target of GSH synthesis, SLC7A11, its expression was rather unaffected in A-T cells and slightly reduced in WT cells.

Among the genes involved in NADPH production, G6PD was found to be overexpressed in all tested LCLs, but significantly overexpressed only in A-T cells. PHGDH overexpression was confirmed in AT129RM, but not in AT50RM or AT28RM, while it was downregulated in WT. ME1 and IDH1 were rather unaffected. Taken together, these results showed an overall transactivation of antioxidant genes giving rise to the hypothesis that Dexa could somehow turn on the different targets by means of one or more specific mechanisms.

The groups of antioxidant genes are jointly regulated by a single transcription factor, NRF2, which is encoded by the *NFE2L2* gene. Therefore, we first assessed the transcriptional activation of *NFEL2L2* by quantitative PCR. **FIGURE 5A** displays how Dexa elicited a mild induction in A-T cells after 24-hour Dexa treatment but not in WT cells but the difference is not statistically significant. However, NRF2 activation mainly occurs at the protein level and is regulated by a fine-tuned mechanism [46]. Under resting conditions, NRF2 is continuously degraded in the cytoplasm by its suppressor KEAP1. In response to stress, NRF2 is released from its suppressor, leading to protein translocation and accumulation in the nucleus. Hence, we assessed the nuclear shift of NRF2 by western blot on cytosolic and nuclear fractions from WT and A-T cells treated with Dexa or untreated. As shown in **FIGURE 5B,** the drug was able to dramatically promote the nuclear translocation of NRF2, especially in A-T cells, as shown by the nuclear accumulation and concomitant disappearance from the cytosol. Moreover, the western blot on total extracts showed no significant changes in the NRF2 protein level, thus excluding that NRF2 nuclear accumulation is a consequence of the overall increase in protein expression (**FIGURE 5C**). Intracellular redistribution of NRF2 was also assayed by immunofluorescence, confirming the nuclear localization only in A-T cells treated with Dexa (**FIGURE 5D** and **5E**). The activation of NRF2 pathway was indeed functionally assessed by Real-Time PCR analysis of a well-characterized NRF2 target gene, NQO1 used as positive control (**FIGURE 5F**).

Hence, our data provide strong evidence that Dexamethasone enhances cellular antioxidant defences via NRF2 activation, which in turn results in transcriptional induction of the antioxidant genes required for the

synthesis of GSH and NADPH. Our next step was then to assess whether the increased transcriptional rate was accompanied by a parallel increase in enzymatic activity and/or metabolic rate.

Effect of Dexa on antioxidant enzymes and metabolic pathways

The production of two of the most abundant antioxidants, NADPH and GSH, has been shown to be positively modulated by Dexa in A-T cells. The above-mentioned data are consistent with an increase in glutathione synthesis, driven by NRF2-dependent overexpression of GSH biosynthetic enzymes. Among the NADPH-producing enzymes, we demonstrated that Dexa may enhance NADPH production via induction of glucose 6-phosphate dehydrogenase (G6PD). G6PD is the rate limiting enzyme of the pentose phosphate pathway (PPP), which is the key pathway for NADPH generation, accounting for approximately 60% of total NADPH production in human cells. Therefore, we investigated whether the higher transcription rate of the G6PD gene was associated with a higher enzymatic activity. G6PD activity was evaluated by spectrophotometric assay. As displayed in **FIGURE 6A**, the activity of the enzyme after Dexamethasone treatment was higher than in untreated cells both in WT and A-T LCLs, as expected by the higher gene transcription, but the increase was significant only in A-T cells. Because G6PD and the NADPH/NADP ratio control the amount of glucose directed to the hexose monophosphate shunt, we decided to investigate whether the higher enzyme activity was associated with an effective higher rate of pathway utilization. Thus, we assessed glucose metabolism and the rate of the PPP in AT129RM cell line before and after Dexa (**FIGURE 6B)**. PPP rates were determined as the difference between the amounts of $^{14}CO_2$ production from the oxidation of [1-$C^{14}$]-glucose, occurring in both the PPP and TCA (first bars) and $CO_2$ production from [6-$C^{14}$]-glucose that, under the experimental conditions, is mainly produced in the Krebs cycle (second bars). The resulting values are represented by the last bars showing that the amount of $^{14}CO_2$ produced during the oxidative decarboxylation of the hexose monophosphate pathway increased after Dexamethasone administration, consistent with an increased rate of the PPP. At the same time, the graph shows that the carbon dioxide produced by oxidative decarboxylation during TCA decreases after Dexamethasone treatment, suggesting a reduced influx of glycolytic products to the mitochondrion. To verify this hypothesis, we assessed the effect of Dexamethasone on the transcription of PDK4, which negatively regulates pyruvate dehydrogenase thereby blocking the influx of pyruvate into TCA. As shown in **FIGURE 6C,** a significant overexpression of PDK4 was found both in WT and A-T cells receiving Dexa, with the latter cells showing a higher increase.

We subsequently investigated whether this metabolic reprogramming could affect the energetic status of A-T cells. To this end, we measured the ATP and NADH levels in WT and A-T cells treated with Dexa or untreated. **FIGURE 7A** shows the intracellular concentration of AMP, ADP and ATP, with no significant differences observed in WT and A-T cells before and after drug administration. On the other hand, as shown in **FIGURE 7B,** there was an increase in NADH levels after Dexa administration, especially in A-T cells, where $NAD^+$ levels also increased slightly.

This result suggested that an enrichment of the NAD pool might contribute to an increase in NADPH. $NAD^+$ can be converted into $NADP^+$ thanks to the action of NAD kinase. We therefore evaluated the effect of Dexa on NADK genes and proteins. NADK induction was first investigated by RT-PCR and then by enzymatic activity in WT and A-T cells with or without Dexa treatment. 24 hours after Dexa administration, no significant effects were detectable in mRNA levels or in enzymatic activity (**FIGURE 8**).

## DISCUSSION

Far from being only a DNA damage kinase relegated to the nucleus, ATM is emerging as a pivotal and ubiquitous kinase, which can be directly activated by oxidative stress. ATM localizes to the cytosol and in particular to organelles such as mitochondria to manage the antioxidant response and orchestrate mitochondrial metabolism, autophagy and the overall cellular metabolism [13;15;18;19;47;48]. In addition, a growing body of evidence suggests that metabolic defects strongly contribute to the complex A-T phenotype observed in patients [10;14;23-25;28;49-51]. Among the impaired metabolic pathways, glucose, purine metabolism and lipid turnover are the most known. On the other hand, as long as the understanding of the role of ATM in A-T physiopathology remains poorly understood, the development of a cure will continue to be elusive. Indeed, effective therapeutic approaches are still lacking, although there is growing interest in steroid treatments (in particular Betamethasone and Dexamethasone) and pharmacological manipulation of the metabolism (http://www.atcp.org/GrantsFunded#sthash.BqE5Zubj.dpuf)**.** In addition, some clinicians are calling for the measurement of GSH levels in the brains of A-T children using current neurological scales for the assessment of neurodegeneration.

In light of the current state of research in the field, we attempted to put some pieces of the puzzle together by investigating whether the therapeutic effectiveness of Dexamethasone on A-T phenotype could be related to redox homeostasis and cell metabolism. To this end, the antioxidant capacity and the metabolic reprogramming after Dexa treatment were investigated in A-T cell models.

Dean [42] was the first author to suggest that GSH metabolism could be involved in the sensitivity of A-T cells to ionizing radiation and DNA damage accumulation. However, he reported that basal GSH levels were similar in A-T and normal fibroblasts. Moreover, he investigated several aspects of glutathione metabolism but found no significant variations in GST activity and only a small reduction in GSR activity. One year later, Meredith and Dodson [45], in agreement with Dean, showed that basal GSH content was similar in fibroblasts and lymphoblasts from A-T patients compared to WT cells. Hence, they hypothesized an impaired glutathione re-synthesis in A-T cells after its depletion. However, their findings were promptly questioned by Dean who stated that a reduced rate of re-synthesis can be found only in some A-T fibroblasts, as it is related to passage number [43]. Our results are consistent with Dean's findings, confirming that neither basal GSH levels in A-T lymphoblasts (31-35 nmol/mg proteins) nor in A-T fibroblasts (15-20 nmol/mg proteins) differ significantly compared to WT. Interestingly, we found that Dexamethasone significantly increases GSH levels in both A-T and WT cells. The only study that examined the effect of betamethasone on oxidative stress in A-T, by Russo et al. [34], inversely correlated antioxidant capacity to cerebellar atrophy and measured GSH levels in peripheral blood mononuclear cells from A-T patients enrolled in a clinical trial, who received a short-term steroid treatment. Unfortunately, GSH measurements after betamethasone treatment were not investigated in this study.

Moreover, we did not find noteworthy abnormalities in glutathione metabolism in A-T cells. In agreement with Dean [42], we revealed that in basal A-T cells, GSH accounted for 90-95% of total glutathione. In contrast, Degan et al. documented a significant decrease in GSSG content in A-T patients suggesting an adaptive response to pro-oxidants [44]. We demonstrated that Dexa was able to increase total glutathione without affecting oxidized glutathione. Glutathione reductase contributes to increase reduced but not total glutathione by regenerating GSH from GSSG after its utilization during ROS scavenging. Accordingly, a slight but insignificant increase in GSR expression was observed in A-T cells. Moreover, we showed that after Dexa treatment, A-T cells exhibit GSH levels that are even higher than those in basal WT cells, suggesting that the drug strengthens the antioxidant capacity of A-T cells, perhaps as an adaptive mechanism to chronic oxidative stress, as hypothesized by Degan [44]. Overall, these data are consistent with a rise in glutathione *de novo* synthesis. As reported in **TABLE 2**, the synthesis of the tri-peptide GSH occurs in two subsequent reactions, and it is mainly regulated via the activity of glutamyl-cysteine ligase (GCL), the enzyme which catalyses the first critical gamma-peptide bond formation between glutamate and

cysteine [52]. We showed that that Dexa significantly enhanced GCL and glutathione synthetase (GSS) expression in A-T cells by quantitative PCR. Both the catalytic and modifier subunits of GCL are regulated at multiple levels to activate GSH biosynthesis, and up-regulation of GSS can further enhance the capacity of cells to synthetize glutathione [52]. The last determinant in glutathione biosynthesis is the availability of cysteine in the cells. We found a slightly higher level of SLC7A11 mRNA in WT cells compared to A-T cells; nevertheless, its expression was unaffected by Dexa. This gene encodes for the cysteine/glutamate carrier, which transports cysteine in exchange for glutamate, thereby contributing to the availability of cysteine in the cells. Meredith et al. suggested an impaired cystine uptake in A-T fibroblasts [45], but, as already mentioned, these findings were questioned by Dean et al. [42]. More recently, Campbell et al. reported a decreased expression of XCT transporter in astroglia culture from A-T mice [41]. We have found intracellular cysteine levels to be similar in WT and A-T lymphoblastoid cells, and slightly increased in both after Dexa administration (data not shown), although cysteine transporter transcription was unaffected. However, it is noteworthy that the cysteine level is not limited to cysteine import but is also generated by transulfuration of methionine, and this is particularly true in high GSH utilising cells such as lymphocytes [53]. Moreover, a recent work hypothesizes that depletion of cystathionine gamma-lyase, the enzyme responsible for cysteine production from cystathionine in the transulfuration pathway, may mediate neurodegeneration in Hungtinton's disease [54].

Concomitant with the GSH increase, an increase in NADPH content was observed in both WT and A-T lymphoblastoid cells after 24h Dexa treatment. Among the targets involved in NADPH production, we found that Dexa significantly trans-activated only the G6PD gene. Enhanced G6PD transcription was accompanied by a parallel increase in enzyme activity. Other authors have previously observed a positive effect of Dexa on G6PD mRNA [55] and protein [56;57]. Increased G6PD activity, in addition to leading to direct production of NADPH, prompts glucose metabolism in the pentose phosphate pathway. The third reaction of PPP catalysed by phosphogluconate dehydrogenase can further increase NADPH production. The activity of this enzyme has also been assayed, but no significant increase was found in WT or AT129 RM cells (data not shown).

In summary, Dexa proved able to increase the production of two of the most abundant antioxidants, GSH and NADPH, thereby improving the antioxidant capacity of A-T cells to counteract oxidative stress. NRF2 acts as master regulator of the antioxidant response driving the expression of most of the antioxidant genes, including those involved in GSH and NAPDH production [58]. Thus, we hypothesized that Dexa could strengthen the cellular antioxidant defences by triggering this antioxidant machinery. We showed that in A-T cells, NRF2 is shifted by Dexa from cytosol to the nucleus, where its accumulation continues up to 24-h after drug administration to sustain phase II antioxidant gene expression. In WT cells, NRF2 is also involved in enhancing antioxidants but is probably rapidly inactivated, as demonstrated by the transcription of target genes which is inhibited at 24h. Unfortunately, we cannot provide conclusive evidence of the critical role of NRF2 because NRF2 mRNA silencing, which would have been the most recommended approach, is not viable owing to inefficient transfection of lymphoblastoid cells. However, additional experiments to explore in depth the role and modes of activation of NRF2 are ongoing.

The production of NAPDH is closely related to cellular metabolism, as it is produced within cells via glucose and glutamine metabolism. Indeed, Glucose 6-phosphate is a key regulatory checkpoint in the overall glucose metabolism. Under normal conditions, 90% of glucose is directed to glycolysis while only 10% is directed to the pentose phosphate pathway (PPP). Under oxidative stress conditions, the rate of PPP can be dramatically increased to promote antioxidant defence [59] and DNA repair [7]. We found that Dexa was indeed able to increase the PPP rate in A-T cells. Moreover, a lower influx of glycolytic intermediates to TCA was shown. Hence, we investigated whether this metabolic reprogramming involved reduced activity of pyruvate dehydrogenase, a key regulatory checkpoint in the carbohydrate metabolism. Pyruvate dehydrogenase is negatively regulated by pyruvate dehydrogenase kinase in response to various stimuli. Several isoforms exist for this enzyme, and among these, we focused on PDK4, which acts in response to

metabolic stress to switch metabolism from glucose to fatty acids to preserve glucose. In addition, PDK4 is known to be trans-activated by glucocorticoids [60]. Effectively, PDK4 was shown to be significantly induced by Dexa in both WT and A-T cells. As mentioned above, inhibition of pyruvate dehydrogenase reduces pyruvate metabolism in the mitochondrion with a decreased mitochondrial ROS production. Interestingly, in response to ROS, ATM inhibits oxidative phosphorylation through the AMPK and HIFα pathways, thus reducing mitochondrial ROS production [50]. Indeed, activated ATM promotes an overall energy metabolism reprogramming to maintain cellular redox homeostasis. It is well known that oxidized ATM activates multiple redox signalling pathways to increase the cellular antioxidant capacity (for example, enhancing glycolysis by up-regulating glucose uptake via AKT-dependent manner) and to promote the pentose phosphate pathway via G6PD activation, increasing NADPH generation [50]. In the absence of ATM, we showed that Dexa can drive this metabolic reprogramming in response to an increased requirement of NADPH, which suggests that this gain in functions could be mediated by protein replacement. Indeed, in a previous work performed on the same cell lines [39], we demonstrated that Dexa promotes the production of a shortened but active ATM protein variant. Moreover, the activation of NRF2 may be related to ATM kinase activity. Some authors are proposing new ways of regulation of NRF2 managed by key kinases such as AKT, ERK and p38 MAPK [61] that are at the moment under our investigations.

Finally, unlike other Authors [62;63], we did not find lower ATP or NAD levels in untreated A-T cells compared to WT cells, but previous evidence was based on experiments in the brain of *ATM*$^{-/-}$ mice and primary A-T fibroblasts. In lymphoblasts, we showed that even though Dexa reduces the entrance of glycolytic metabolites to the TCA this does not affect significantly ATP and NADH contents. We can speculate that diverging glucose from the TCA, the cellular machinery is forced to fall back on glutamine to draw energy. Glutamine enters the TCA directly at the level of alpha-ketoglutarate and is able to fully sustain the energetic requirement of the cells in terms of ATP and NADH. Preliminary microarray data performed in our cellular models show that oxoglutarate (alpha-ketoglutarate) dehydrogenase, the enzyme which regulates the flux of glutamine into the TCA, is one of the most over-expressed genes after Dexa administration. Conversely, we observed that NAPDH content was more affected by the drug. Then, we hypothesized the involvement of a metabolic network between the synthesis of NADH and NADPH. NAD kinase converts NAD to NADP, and its role in energy metabolism [64] and antioxidant defence is emerging [65]. Nonetheless, investigations of this kinase did not show any significant effect by Dexa. This is consistent with Pollak's work [65] indicating that NADK is summoned only when the NADP pool is significantly diminished thus becoming the limiting factor. That is to say, the rate of NADPH regeneration is more critical than the actual concentration of the pre-existing NADPH.

In conclusion, in this work we propose a novel role for glucocorticoid as a guest actor in the antioxidant pathway in Ataxia Telangiectasia. Regardless of whether this effect relies on direct or indirect mechanisms, our results mark a step forward in the understanding of steroid action in neurodegenerative diseases and suggest that the drug may be much more than a simple anti-inflammatory or immunosuppressive compound.

## MATERIAL AND METHODS

### *Cell lines*

Lymphoblastoid cell lines (LCLs) used in this study were AT50RM, AT28RM, AT129RM, derived from three A-T patients ($ATM^{-/-}$), whose genotype is reported in **TABLE 1**, and one wild type donor ($ATM^{+/+}$), as control. All cell lines were established from fresh lymphocytes infected by Epstein-Barr virus and maintained in RPMI1640 medium supplemented with 2 mM L-glutamine, 100 U/mL Penicillin, 0.1 mg/mL Streptomycin, and 10% fetal bovine serum.

Human primary fibroblasts, AG09429 ($ATM^{+/+}$) and GM2052 ($ATM^{-/-}$) (Coriell Institute, Camden, USA), were grown in Minimum Essential Medium Eagle. The medium was supplemented with 2 mM L-glutamine, 100 U/mL Penicillin, 0.1 mg/mL Streptomycin, 10% FBS (for AG09429) and 15% FBS (for GM2052).

All cells were incubated at 37°C with 5% $CO_2$ and treated with 100 nM Dexa for 24h prior to metabolite, RNA and protein extractions. Dimethylsulfoxide (DMSO) was used as the drug vehicle and thus administered in untreated cells as a control.

### *Measurement of reducing equivalents*

The endogenous levels of reduced glutathione (GSH) in WT and A-T lymphoblastoid cell lines treated or not with Dexa were measured as previously reported [66]. 1 x $10^6$ cells were washed twice in PBS and immediately subjected to lysis and protein precipitation. De-proteinized supernatants were added with 25% (v/v) $Na_2HPO_4$ and 10% (v/v) DTNB and used for HPLC determination of derivatized thiols. Quantitative measurements were obtained by injection of standard solutions of GSH. In some cases, the same thiol extracts were used for determination of total glutathione. Briefly, samples were added with suitable concentrations of NADPH, DTNB and GSH reductase to convert oxidized glutathione into GSH, according to [67]. Total glutathione was then quantified by spectrophotometric assay at 412 nm as described in [68]. Nicotinamide adenine dinucleotide phosphate is an enzymatic cofactor involved in many redox reactions where it cycles between the reduced (NADPH) and the oxidized ($NADP^+$) forms. $NADP^+$and NADPH were extracted from lymphoblastoid cells and measured using a colorimetric assay ($NADP^+$/NADPH Quantitation Kit, Sigma Aldrich).

### ROS measurements

Cellular ROS were evaluated by 2',7'-dichlorofluorescein diacetate (DFCH-DA) assay [69]. DCFH-DA (Sigma Aldrich) is a nonfluorescent compound that reacts with cellular ROS to produce dichlorofluorescein (DCF), a highly fluorescent molecule. 5 µM of DCFH-DA was administered to 1 x $10^6$ WT and A-T lymphoblastoid cells treated or not with Dexamethasone and incubated for 20 min at 5% $CO_2$, essentially as described in [34]. Cells were collected, washed with PBS and immediately analysed on a microplate assay.

### *Quantitative Real-Time PCR*

Total RNA was extracted from LCLs treated or not treated with Dexa, using the RNeasy mini kit (Qiagen) and cDNA was obtained by PowerScript reverse transcriptase (Clontech). Quantitative PCRs were performed by custom TaqMan® Array Plates 16 x 6 Format (Life Technologies). The selected targets are listed in **TABLE 2** with a brief description of their role in the antioxidant response. *18S* and *HPRT1* were used as housekeeping genes. Positive target validations, as well as other quantitative PCRs, were performed by the respective single-tube assay TaqMan® Gene Expression Assay (Life Technologies).

*Western blotting and fluorescence imaging*

Western blots were performed on WT and A-T cytosolic and nuclear protein extracts. Antibodies used in the analyses were anti-NRF2 and anti-HPRT1, from Santa Cruz Biotechnology, and anti-Lamin A/C, from Diatheva. Microscopic observations of NRF2 were performed by Leica DMLB fluorescent microscope equipped with a DC300F CCD camera. Images were analysed by ImageJ as reported in [70]. NRF2 normalised signals were integrated by using the DAPI signal as ROI. About 250 cells were counted for each sample.

*Enzyme activity assays*

Glucose 6-phosphate dehydrogenase (G6PD) activity was evaluated by spectrophotometric assays reported by [71]. G6PD catalyses the oxidation of glucose 6-P to 6-phosphogluconolactone, which spontaneously hydrolyses to 6-phosphogluconate (PGA) generating one mole of NADPH. 6-phosphogluconate dehydrogenase (6PGD) catalyzes the oxidation of the newly formed 6-PGA to ribulose 5-phosphate with the production of another mole of NADPH.

$$\text{GLUCOSE 6-P} + \text{NAPD}^{+} \xrightarrow{G6PD} \text{6-PGA} + \text{NADPH} + \text{H}^{+}$$

$$\text{6-PGA} + \text{NADP}^{+} \xrightarrow{6PGD} \text{RIBULOSE 5-P} + \text{CO}_2 + \text{NADPH} + \text{H}^{+}$$

Measurements were made by monitoring the increase in absorption at 340 nm due to the reduction of $NADP^+$ to NADPH at 37°C. One enzyme unit represents the reduction of 1 μmol of $NADP^+$/min. Also phosphogluconate dehydrogenase (PGD) was assayed as described in [72].

NAD kinase (NADK) activity was measured essentially as described in [73]. NADK catalyses the conversion of $NAD^+$ to $NADP^+$ using ATP as phosphate group donor.

$$\text{NAD}^{+} + \text{ATP} \xrightarrow{NADK} \text{NADP}^{+} + \text{ADP}$$

$$\text{NADP}^{+} + \text{GLUCOSE 6-P} \xrightarrow{G6DP} \text{6-PGA} + \text{NADPH} + \text{H}^{+}$$

Briefly, phosphorylation of $NAD^+$ by NADK was monitored at 340 nm by pairing this reaction with the subsequent reduction of newly formed $NADP^+$ to NADPH by G6PD. Reactions contained 5 mM $NAD^+$, 5 mM ATP, 5 mM glucose 6-phosphate, 0.5 U G6PD (Sigma Aldrich), 5 mM $MgCl_2$ and 100 mM Tris-HCl pH 8.0. All assays were performed on native protein extracts from WT and A-T lymphoblastoid cell lines treated with Dexa or untreated.

*Pentose phosphate pathway rate and overall glucose metabolism*

The pentose phosphate pathway (PPP) rate was determined by incubating cells with tracer doses of [1-$C^{14}$]-glucose and [6-$C^{14}$]-glucose, essentially as reported by [59]. After its internalization, glucose is rapidly phosphorylated to glucose 6-phosphate (G6P) to enter glycolysis. G6P can also be shunted to PPP. In the oxidative branch of PPP, it is first oxidized to 6-phosphogluconate and then decarboxylated to ribulose 5-phosphate. Emission of $CO_2$ can be monitored by administration of radiolabelled glucose in position 1. Glucose 6-phosphate, which continues with glycolysis, can enter the tricarboxylic acid cycle (TCA) encountering two subsequent decarboxylations. Emissions of $CO_2$ during TCA can be monitored by administration of radiolabelled glucose in position 6. The PPP rate was calculated as the difference between the $^{14}CO_2$ derived from [1-$C^{14}$]-glucose (metabolized in both PPP and TCA) and that derived from [6-$C^{14}$]-

glucose (metabolized only by the TCA). Cells were cultured and the assay was performed in 2 mmol/l glucose. Trapping of the $^{14}CO_2$ and scintillation counting were performed as already reported in [74].

*Adenine and pyridine simultaneous extraction and determination*

Determination of ATP, ADP, AMP, $NAD^+$ and NADH in lymphoblastoid cells lines treated with Dexa or untreated was performed by alkaline extraction allowing the simultaneous recovery of purine nucleotides as described in [75]. Nucleotide extraction was followed by chromatographic separation using an ion-pair reverse-phase HPLC method with UV detection developed in our lab [76]. Standard solutions of nucleotides were used for absolute quantitation.

## ACKNOWLEDGMENTS

This work was jointly funded by Sparks, A-T Society and Action for A-T (Grant ref. 14SAP01). We thank FanoAteneo and "Associazione Nazionale A-T Davide De Marini" for their sponsorship.

## AUTHOR CONTRIBUTIONS

SBi conceived and coordinated the study, wrote the paper and performed most of experiments. MMe provided assistance to analysis of data, preparation of the FIGUREs, and executed immunofluorescence experiments in FIGURE 4. AF and SBr contributed to glutathione measurements in FIGURE 1. CS performed the experiments shown in FIGURE 2 and contributed to quantitative PCR analyses shown in FIGURE 6 and 8. MB and SO performed lymphoblast and fibroblast cultures, respectively. LR, LC and MMa gave substantial contributions in study design, discussion and interpretation of data. All authors reviewed the results and approved the final version of the manuscript.

## REFERENCES


[1] Abraham RT (2001) Cell cycle checkpoint signaling through the ATM and ATR kinases. *Genes Dev* 15**,** 2177-2196.

[2] Abraham RT (2004) PI 3-kinase related kinases: 'big' players in stress-induced signaling pathways. *DNA Repair (Amst)* 3**,** 883-887.

[3] Bensimon A, Aebersold R, & Shiloh Y (2011) Beyond ATM: the protein kinase landscape of the DNA damage response. *FEBS Lett* 585**,** 1625-1639.

[4] Boohaker RJ & Xu B (2014) The versatile functions of ATM kinase. *Biomed J* 37**,** 3-9.

[5] Shiloh Y & Ziv Y (2012) The ATM protein: the importance of being active. *J Cell Biol* 198**,** 273-275.

[6] Shiloh Y & Ziv Y (2013) The ATM protein kinase: regulating the cellular response to genotoxic stress, and more. *Nat Rev Mol Cell Biol* 14**,** 197-210.

[7] Cosentino C, Grieco D, & Costanzo V (2011) ATM activates the pentose phosphate pathway promoting anti-oxidant defence and DNA repair. *EMBO J* 30**,** 546-555.

[8] Ditch S & Paull TT (2012) The ATM protein kinase and cellular redox signaling: beyond the DNA damage response. *Trends Biochem Sci* 37**,** 15-22.

[9] Guo Z, Kozlov S, Lavin MF, Person MD, & Paull TT (2010) ATM activation by oxidative stress. *Science* 330**,** 517-521.

[10] Ito K, Hirao A, Arai F, Matsuoka S, Takubo K, Hamaguchi I, Nomiyama K, Hosokawa K, Sakurada K, Nakagata N, Ikeda Y, Mak TW, & Suda T (2004) Regulation of oxidative stress by ATM is required for self-renewal of haematopoietic stem cells. *Nature* 431**,** 997-1002.

[11] Paull TT (2015) Mechanisms of ATM Activation. *Annu Rev Biochem* .

[12] Tang D, Wu D, Hirao A, Lahti JM, Liu L, Mazza B, Kidd VJ, Mak TW, & Ingram AJ (2002) ERK activation mediates cell cycle arrest and apoptosis after DNA damage independently of p53. *J Biol Chem* 277**,** 12710-12717.

[13] Zhang J, Tripathi DN, Jing J, Alexander A, Kim J, Powell RT, Dere R, Tait-Mulder J, Lee JH, Paull TT, Pandita RK, Charaka VK, Pandita TK, Kastan MB, & Walker CL (2015) ATM functions at the peroxisome to induce pexophagy in response to ROS. *Nat Cell Biol* 17**,** 1259-1269.

[14] Takagi M, Uno H, Nishi R, Sugimoto M, Hasegawa S, Piao J, Ihara N, Kanai S, Kakei S, Tamura Y, Suganami T, Kamei Y, Shimizu T, Yasuda A, Ogawa Y, & Mizutani S (2015) ATM Regulates Adipocyte Differentiation and Contributes to Glucose Homeostasis. *Cell Rep* .

[15] Alexander A, Cai SL, Kim J, Nanez A, Sahin M, Maclean KH, Inoki K, Guan KL, Shen J, Person MD, Kusewitt D, Mills GB, Kastan MB, & Walker CL (2010) ATM signals to TSC2 in the cytoplasm to regulate mTORC1 in response to ROS. *Proc Natl Acad Sci U S A* 107**,** 4153-4158.

[16] Ambrose M & Gatti RA (2013) Pathogenesis of ataxia-telangiectasia: the next generation of ATM functions. *Blood* 121**,** 4036-4045.

[17] Kim J & Wong PK (2009) Loss of ATM impairs proliferation of neural stem cells through oxidative stress-mediated p38 MAPK signaling. *Stem Cells* 27**,** 1987-1998.

[18] Valentin-Vega YA, Maclean KH, Tait-Mulder J, Milasta S, Steeves M, Dorsey FC, Cleveland JL, Green DR, & Kastan MB (2012) Mitochondrial dysfunction in ataxia-telangiectasia. *Blood* 119**,** 1490-1500.

[19] Valentin-Vega YA & Kastan MB (2012) A new role for ATM: regulating mitochondrial function and mitophagy. *Autophagy* 8**,** 840-841.

[20] Ambrose M, Goldstine JV, & Gatti RA (2007) Intrinsic mitochondrial dysfunction in ATM-deficient lymphoblastoid cells. *Hum Mol Genet* 16**,** 2154-2164.

[21] Chen P, Peng C, Luff J, Spring K, Watters D, Bottle S, Furuya S, & Lavin MF (2003) Oxidative stress is responsible for deficient survival and dendritogenesis in purkinje neurons from ataxia-telangiectasia mutated mutant mice. *J Neurosci* 23**,** 11453-11460.

[22] D'Souza AD, Parish IA, Krause DS, Kaech SM, & Shadel GS (2013) Reducing mitochondrial ROS improves disease-related pathology in a mouse model of ataxia-telangiectasia. *Mol Ther* 21**,** 42-48.

[23] Kamsler A, Daily D, Hochman A, Stern N, Shiloh Y, Rotman G, & Barzilai A (2001) Increased oxidative stress in ataxia telangiectasia evidenced by alterations in redox state of brains from Atm-deficient mice. *Cancer Res* 61**,** 1849-1854.

[24] Liu N, Stoica G, Yan M, Scofield VL, Qiang W, Lynn WS, & Wong PK (2005) ATM deficiency induces oxidative stress and endoplasmic reticulum stress in astrocytes. *Lab Invest* 85**,** 1471-1480.

[25] Watters DJ (2003) Oxidative stress in ataxia telangiectasia. *Redox Rep* 8**,** 23-29.

[26] Chessa L (2014) Current and future therapeutic strategies to treat ataxia telangiectasia. *Expert Opinion in Orphan Drugs* .

[27] Lee SA, Lee KM, Lee SJ, Yoo KY, Park SK, Noh DY, Ahn SH, & Kang D (2010) Antioxidant vitamins intake, ataxia telangiectasia mutated (ATM) genetic polymorphisms, and breast cancer risk. *Nutr Cancer* 62**,** 1087-1094.

[28] da SR, dos Santos-Valente EC, Burim SF, Saccardo Sarni RO, & Costa-Carvalho BT (2014) The relationship between nutritional status, vitamin A and zinc levels and oxidative stress in patients with ataxia-telangiectasia. *Allergol Immunopathol (Madr )* 42**,** 329-335.

[29] Broccoletti T, Del GE, Amorosi S, Russo I, Di BM, Imperati F, Romano A, & Pignata C (2008) Steroid-induced improvement of neurological signs in ataxia-telangiectasia patients. *Eur J Neurol* 15**,** 223-228.

[30] Broccoletti T, Del GE, Cirillo E, Vigliano I, Giardino G, Ginocchio VM, Bruscoli S, Riccardi C, & Pignata C (2011) Efficacy of very-low-dose betamethasone on neurological symptoms in ataxia-telangiectasia. *Eur J Neurol* 18**,** 564-570.

[31] Buoni S, Zannolli R, Sorrentino L, & Fois A (2006) Betamethasone and improvement of neurological symptoms in ataxia-telangiectasia. *Arch Neurol* 63**,** 1479-1482.

[32] Chessa L, Leuzzi V, Plebani A, Soresina A, Micheli R, D'Agnano D, Venturi T, Molinaro A, Fazzi E, Marini M, Ferremi LP, Quinti I, Cavaliere FM, Girelli G, Pietrogrande MC, Finocchi A, Tabolli S, Abeni D, & Magnani M (2014) Intra-erythrocyte infusion of dexamethasone reduces neurological symptoms in ataxia teleangiectasia patients: results of a phase 2 trial. *Orphanet J Rare Dis* 9**,** 5.

[33] Quarantelli M, Giardino G, Prinster A, Aloj G, Carotenuto B, Cirillo E, Marsili A, Salvatore E, Del GE, & Pignata C (2012) Steroid treatment in Ataxia-Telangiectasia induces alterations of functional magnetic resonance imaging during prono-supination task. *Eur J Paediatr Neurol* .

[34] Russo I, Cosentino C, Del GE, Broccoletti T, Amorosi S, Cirillo E, Aloj G, Fusco A, Costanzo V, & Pignata C (2009) In ataxia-teleangiectasia betamethasone response is inversely correlated to cerebellar atrophy and directly to antioxidative capacity. *Eur J Neurol* 16**,** 755-759.

[35] Zannolli R, Sabrina B, Betti G, Salvucci S, Plebani A, Soresina A, Pietrogrande MC, Martino S, Leuzzi V, Finocchi A, Micheli R, Rossi LN, Brusco A, Misiani F, Fois A, Hayek J, Kelly C, & Chessa L (2012) A randomized trial of oral betamethasone to reduce ataxia symptoms in ataxia telangiectasia. *Mov Disord* 27**,** 1312-1316.

[36] Leuzzi V, Micheli R, D'Agnano D, Molinaro A, Venturi T, Plebani A, Soresina A, Marini M, Ferremi LP, Quinti I, Pietrogrande MC, Finocchi A, Fazzi E, Chessa L, & Magnani M (2015) Positive effect of erythrocyte-delivered dexamethasone in ataxia-telangiectasia. *Neurol Neuroimmunol Neuroinflamm* 2**,** e98.

[37] Gatti RA & Perlman S (2009) A proposed bailout for A-T patients? *Eur J Neurol* 16**,** 653-655.

[38] Giardino G, Fusco A, Romano R, Gallo V, Maio F, Esposito T, Palamaro L, Parenti G, Salerno MC, Vajro P, & Pignata C (2013) Betamethasone therapy in ataxia telangiectasia: unraveling the rationale of this serendipitous observation on the basis of the pathogenesis. *Eur J Neurol* 20**,** 740-747.

[39] Menotta M, Biagiotti S, Bianchi M, Chessa L, & Magnani M (2012) Dexamethasone partially rescues ataxia telangiectasia-mutated (ATM) deficiency in ataxia telangiectasia by promoting a shortened protein variant retaining kinase activity. *J Biol Chem* 287**,** 41352-41363.

[40] Biagiotti S, Menotta M, Giacomini E, Radici L, Bianchi M, Bozzao C, Chessa L, & Magnani M (2014) Forward subtractive libraries containing genes transactivated by dexamethasone in ataxia-telangiectasia lymphoblastoid cells. *Mol Cell Biochem* .

[41] Campbell A, Bushman J, Munger J, Noble M, Proschel C, & Mayer-Proschel M (2015) Mutation of ataxia-telangiectasia mutated is associated with dysfunctional glutathione homeostasis in cerebellar astroglia. *Glia* .

[42] Dean SW (1987) Some aspects of glutathione metabolism in ataxia-telangiectasia fibroblasts. *Int J Radiat Biol Relat Stud Phys Chem Med* 52**,** 43-48.

[43] Dean SW, Sykes HR, Cole J, Jaspers NG, Linssen P, & Verkerk A (1988) Re: Impaired glutathione biosynthesis in cultured ataxia-telangiectasia cells. *Cancer Res* 48**,** 5374-5376.

[44] Degan P, d'Ischia M, Pallardo FV, Zatterale A, Brusco A, Calzone R, Cavalieri S, Kavakli K, Lloret A, Manini P, Pisanti MA, Vuttariello E, & Pagano G (2007) Glutathione levels in blood from ataxia telangiectasia patients suggest in vivo adaptive mechanisms to oxidative stress. *Clin Biochem* 40**,** 666-670.

[45] Meredith MJ & Dodson ML (1987) Imparied glutathione biosynthesis in cultured human ataxia-telangiectasia cells. *Cancer Res* 47**,** 4576-4581.

[46] Anuranjani & Bala M (2014) Concerted action of Nrf2-ARE pathway, MRN complex, HMGB1 and inflammatory cytokines - implication in modification of radiation damage. *Redox Biol* 2**,** 832-846.

[47] Lim DS, Kirsch DG, Canman CE, Ahn JH, Ziv Y, Newman LS, Darnell RB, Shiloh Y, & Kastan MB (1998) ATM binds to beta-adaptin in cytoplasmic vesicles. *Proc Natl Acad Sci U S A* 95**,** 10146-10151.

[48] Watters D, Kedar P, Spring K, Bjorkman J, Chen P, Gatei M, Birrell G, Garrone B, Srinivasa P, Crane DI, & Lavin MF (1999) Localization of a portion of extranuclear ATM to peroxisomes. *J Biol Chem* 274**,** 34277-34282.

[49] Barzilai A, Rotman G, & Shiloh Y (2002) ATM deficiency and oxidative stress: a new dimension of defective response to DNA damage. *DNA Repair (Amst)* 1**,** 3-25.

[50] Tang S, Yang L, Tang X, & Liu M (2014) The role of oxidized ATM in the regulation of oxidative stress-induced energy metabolism reprogramming of CAFs. *Cancer Lett* 353**,** 133-144.

[51] Halaby MJ, Hibma JC, He J, & Yang DQ (2008) ATM protein kinase mediates full activation of Akt and regulates glucose transporter 4 translocation by insulin in muscle cells. *Cell Signal* 20**,** 1555-1563.

[52] Lu SC (2009) Regulation of glutathione synthesis. *Mol Aspects Med* 30**,** 42-59.

[53] Iglehart JK, York RM, Modest AP, Lazarus H, & Livingston DM (1977) Cystine requirement of continuous human lymphoid cell lines of normal and leukemic origin. *J Biol Chem* 252**,** 7184-7191.

[54] Paul BD & Snyder SH (2014) Neurodegeneration in Huntington's disease involves loss of cystathionine gamma-lyase. *Cell Cycle* 13**,** 2491-2493.

[55] Kletzien RF, Harris PK, & Foellmi LA (1994) Glucose-6-phosphate dehydrogenase: a "housekeeping" enzyme subject to tissue-specific regulation by hormones, nutrients, and oxidant stress. *FASEB J* 8**,** 174-181.

[56] Karaman K, Tirnaksiz MB, Ulusu N, Dincer N, Sener B, Gulmez D, Tandogan B, Sokmensuer C, & Sayek I (2011) Effects of dexamethasone on ischemia reperfusion injury following pringle maneuver. *Hepatogastroenterology* 58**,** 465-471.

[57] Rosa LF, Cury Y, & Curi R (1992) Effects of insulin, glucocorticoids and thyroid hormones on the activities of key enzymes of glycolysis, glutaminolysis, the pentose-phosphate pathway and the Krebs cycle in rat macrophages. *J Endocrinol* 135**,** 213-219.

[58] Gorrini C, Harris IS, & Mak TW (2013) Modulation of oxidative stress as an anticancer strategy. *Nat Rev Drug Discov* 12**,** 931-947.

[59] Takahashi S, Izawa Y, & Suzuki N (2012) Astroglial pentose phosphate pathway rates in response to high-glucose environments. *ASN Neuro* 4.

[60] Connaughton S, Chowdhury F, Attia RR, Song S, Zhang Y, Elam MB, Cook GA, & Park EA (2010) Regulation of pyruvate dehydrogenase kinase isoform 4 (PDK4) gene expression by glucocorticoids and insulin. *Mol Cell Endocrinol* 315**,** 159-167.

[61] Buendia I, Michalska P, Navarro E, Gameiro I, Egea J, & Leon R (2016) Nrf2-ARE pathway: An emerging target against oxidative stress and neuroinflammation in neurodegenerative diseases. *Pharmacol Ther* 157**,** 84-104.

[62] Marecki JC & McCord JM (2002) The inhibition of poly(ADP-ribose) polymerase enhances growth rates of ataxia telangiectasia cells. *Arch Biochem Biophys* 402**,** 227-234.

[63] Stern N, Hochman A, Zemach N, Weizman N, Hammel I, Shiloh Y, Rotman G, & Barzilai A (2002) Accumulation of DNA damage and reduced levels of nicotine adenine dinucleotide in the brains of Atm-deficient mice. *J Biol Chem* 277**,** 602-608.

[64] Ying W (2008) NAD+/NADH and NADP+/NADPH in cellular functions and cell death: regulation and biological consequences. *Antioxid Redox Signal* 10**,** 179-206.

[65] Pollak N, Niere M, & Ziegler M (2007) NAD kinase levels control the NADPH concentration in human cells. *J Biol Chem* 282**,** 33562-33571.

[66] Fraternale A, Crinelli R, Casabianca A, Paoletti MF, Orlandi C, Carloni E, Smietana M, Palamara AT, & Magnani M (2013) Molecules altering the intracellular thiol content modulate NF-kB and STAT-1/IRF-1 signalling pathways and IL-12 p40 and IL-27 p28 production in murine macrophages. *PLoS One* 8**,** e57866.

[67] Pujari G, Berni A, Palitti F, & Chatterjee A (2009) Influence of glutathione levels on radiation-induced chromosomal DNA damage and repair in human peripheral lymphocytes. *Mutat Res* 675**,** 23-28.

[68] Beutler E (1984) Reduced glutathione. In *Red Cell Metabolism. A Manual of Biochemical Methods* (Grune & Stratton, ed), pp. 131-133. Orlando, FL.

[69] Rosenkranz AR, Schmaldienst S, Stuhlmeier KM, Chen W, Knapp W, & Zlabinger GJ (1992) A microplate assay for the detection of oxidative products using 2',7'-dichlorofluorescin-diacetate. *J Immunol Methods* 156**,** 39-45.

[70] Schneider CA, Rasband WS, & Eliceiri KW (2012) NIH Image to ImageJ: 25 years of image analysis. *Nat Methods* 9**,** 671-675.

[71] Beutler E (1984) Glucose-6-phosphate dehydrogenase and 6-phosphogluconate dehydrogenase. In *Red Cell Metabolism. A Manual of Biochemical Methods* pp. 68-71. Grune & Stratton, Orlando, FL.

[72] GLOCK GE & McLEAN P (1953) Further studies on the properties and assay of glucose 6-phosphate dehydrogenase and 6-phosphogluconate dehydrogenase of rat liver. *Biochem J* 55**,** 400-408.

[73] Love NR, Pollak N, Dolle C, Niere M, Chen Y, Oliveri P, Amaya E, Patel S, & Ziegler M (2015) NAD kinase controls animal NADP biosynthesis and is modulated via evolutionarily divergent calmodulin-dependent mechanisms. *Proc Natl Acad Sci U S A* 112**,** 1386-1391.

[74] Magnani M, Chiarantini L, Stocchi V, Dacha M, & Fornaini G (1986) Glucose metabolism in fibroblasts from patients with erythrocyte hexokinase deficiency. *J Inherit Metab Dis* 9**,** 129-139.

[75] Stocchi V, Cucchiarini L, Magnani M, Chiarantini L, Palma P, & Crescentini G (1985) Simultaneous extraction and reverse-phase high-performance liquid chromatographic determination of adenine and pyridine nucleotides in human red blood cells. *Anal Biochem* 146**,** 118-124.

[76] Stocchi V, Cucchiarini L, Canestrari F, Piacentini MP, & Fornaini G (1987) A very fast ion-pair reversed-phase HPLC method for the separation of the most significant nucleotides and their degradation products in human red blood cells. *Anal Biochem* 167**,** 181-190.

**TABLE 1. GENOTYPING OF A-T LYMPHOBLASTOID CELL LINES**

| ***LCL*** | **Genotype** | **Mutation allele 1 and resulting protein** | | **Mutation allele 2 and resulting protein** | |
|---|---|---|---|---|---|
| *AT50RM* | Compound Htz | 7792C>T | Nonsense/ Truncated protein | 8283delTC | Deletion/ Truncated protein |
| *AT28RM* | Compound Htz | 5692C>T | Nonsense/ Truncated protein | IVS37+2T>C | Splicing/ Truncated protein |
| *AT129RM* | Hmz | 8283delTC | Deletion/ Truncated protein | 8283delTC | Deletion/ Truncated protein |

Lymphoblastoid cell lines were established both from A-T patients ($ATM^{-/-}$) and healthy volunteers ($ATM^{+/+}$). In the table genotyping of A-T cell lines is reported; as shown, all the investigated mutations lead to truncated protein with no detectable ATM levels.

**TABLE 2. SELECTED GENE TARGETS INVOLVED IN THE ANTIOXIDANT RESPONSE**

| **GSH SYNTHESIS AND REGENERATION** | | **NADPH PRODUCTION** | | **GSH UTILIZATION** | |
|---|---|---|---|---|---|
| *GCLC* | Glutamylcysteine ligase catalytic subunit | *G6PD* | Glucose 6-phosphate dehydrogenase | *GPX2* | Glutathione peroxidase |
| *GCLM* | Glutamylcysteine ligase modifier subunit | *PHGDH* | Phosphoglycerate dehydrogenase | *GSTA1,3,5* | Glutathione transferases |
| *GSS* | Glutathione synthetase | *ME1* | Malic enzyme | | |
| *XCT* | Cysteine transporter | *IDH1* | Isocytrate dehydrogenase | | |
| *GSR* | Glutathione reductase | | | | |

Among the antioxidant pathways we focused on GSH synthesis and regeneration and NADPH production. GSH production is regulated by glutamylcysteine ligase, which catalyses the first step of glutathione *de novo* synthesis, that is the isopeptide bond formation between glutamate and cysteine. The enzyme complex is composed of a catalytic subunit (*GCLC*) and a modifier subunit (*GCLM*). The second step is catalysed by glutathione synthetase (*GSS*), which releases the final tri-peptide after addition of glycine. GSH synthesis is limited by the availability of cysteine into the cells. *SLC7A11* gene encodes for an anionic amino acid carrier (XCT) that transports cysteine in exchange with glutamate, thereby contributing to the intracellular cysteine concentration. Finally, glutathione reductase (*GSR*) participates to GSH homeostasis by regenerating reduced glutathione after oxidation at the cost of a NADPH molecule.

NADPH is mainly produced into the cells by the pentose phosphate pathway that shunts from glycolysis at glucose 6-phosphate level. Glucose-6-phosphate dehydrogenase (*G6PD*) prompts the entrance of glucose 6-phosphate into the oxidative phase of PPP in response to NADPH requirement. Secondarily, NADPH can be formed as a product of metabolic reactions catalysed by malic enzyme 1 (*ME1*) and some isoforms of isocitrate dehydrogenase, such as *IDH1*. This cytoplasmic enzyme serves a significant role in cytoplasmic NADPH production and can localize to the peroxisomes.

Finally, GSH and NADPH productions can be indirectly enhanced by phosphoglycerate dehydrogenase (*PHGDH*), the key enzyme of serine biosynthesis. In fact, serine is the metabolic precursor of glycine, which is needed for GSH synthesis. Moreover, serine affects pyruvate kinase activity leading to the diversion of metabolites from glycolysis towards NADPH generation.

## FIGURE LEGENDS

### FIGURE 1. GSH CONTENT IN WT AND A-T CELLS WITH OR WITHOUT DEXA

(A) Reduced glutathione (GSH) content was evaluated in WT and A-T lymphoblastoid cell lines after 24-hour Dexa and compared with the respective untreated cell line. Values are means and SEM of six independent experiments (Wilcoxon signed rank test; *two-tailed p-values<0.05). (B) Total and reduced glutathione was measured in AT129RM before and after Dexa. Striped bar pattern refers to GSSG obtained by subtracting GSH to total glutathione. (C) GSH contents were evaluated also in WT (AG09429) and A-T (GM2052) fibroblasts, treated or not with Dexa, and subjected to increasing hydrogen peroxide concentrations (0, 25 and 50 μM).

### FIGURE 2. NADPH CONTENT IN WT AND A-T CELLS WITH OR WITHOUT DEXA

(A) NADPH levels and (B) NADPH/NADP+ ratios were evaluated in WT and A-T lymphoblastoid cell lines treated with Dexa and compared with the respective untreated LCLs. Values are means and SD of three independent experiments (Wilcoxon signed rank test; *two-tailed p-values<0.05, **two-tailed p-values<0.005).

### FIGURE 3. ROS LEVEL IN WT AND A-T CELLS WITH OR WITHOUT DEXA

ROS levels were measured by DFCH-DA assay in resting WT and A-T lymphoblastoid cell lines receiving Dexa and compared with the respective untreated cell line. Dashed line represents the threshold of detectability as estimated from the mean of the negative controls. Values are means and SD for quadruplicate wells (Wilcoxon signed rank test; *two-tailed p-values<0.05).

### FIGURE 4. EFFECT OF DEXA ON ANTIOXIDANT GENE EXPRESSION

The effect of Dexa on the gene expression of selected targets belonging to the antioxidant response was evaluated by quantitative PCR. (A) Preliminary time-course analysis performed in AT129RM at 2, 6 and 24 h Dexa. Fold changes were calculated as the difference between the treated and respective untreated sample. (B) Panel of targets in WT and A-T lymphoblastoid cells treated with Dexa for 24 h. Fold changes were calculated as the difference between the treated and respective untreated LCL. Values are means and SEM of four independent experiments. Overexpression has been validated for targets with a *p-value lesser than 0.05 (Wilcoxon signed rank test).

### FIGURE 5. NRF2 GENE EXPRESSION AND PROTEIN LOCALIZATION IN WT AND A-T CELLS WITH OR WITHOUT DEXA

(A) Transactivation of the Nuclear factor 2 gene, *NFE2L2*, was assayed by quantitative PCR. Fold changes were calculated as the difference between the treated and the respective untreated lymphoblastoid cell line. (B) Nuclear shift of NRF2 was assessed by western blot on cytosolic and nuclear fractions extracted from WT and AT129RM treated or not with Dexa. NRF2 protein levels were checked by western blots of total extracts, as well (C). HPRT1 and LAMIN A were used as cytosolic and nuclear loading controls, respectively. Nuclear localization of NRF2 was also confirmed by immunofluorescence imaging (D) and quantification (E) on WT and A-T cells with or without Dexa. (F) The activation of NRF2 was confirmed by Real-Time PCR on NQO1 as positive control. Values are means and SEM of four independent experiments (* = p-values <0.05).

**FIGURE 6. EFFECT OF DEXA ON PENTOSE PHOSPHATE PATHWAY AND OVERALL GLUCOSE METABOLISM**

(A) The activity of G6PD, the rate-limiting enzyme of PPP, was firstly assayed spectrophotometrically on native protein extracts from WT and A-T LCLs treated or not with Dexa. Values are means and SEM of six independent experiments (Wilcoxon signed rank test; *two-tailed p-values<0.05) (B) Effective rates of utilization of PPP was confirmed in AT129RM by administration of [1-$C^{14}$]-glucose and [6-$C^{14}$]-glucose and subsequent monitoring of emitted $^{14}CO_2$. First bars represent the rates of radiolabeled carbon dioxide production by [1-$C^{14}$]-glucose, which is metabolized in both PPP and TCA. Second bars are those produced by [6-$C^{14}$]-glucose metabolized only by the TCA. PPP rates in the last bars were determined as the difference between the rates of $^{14}CO_2$ production from [1-$C^{14}$]- and [6-$C^{14}$]-glucose. Values are means and SEM of six independent experiments (Wilcoxon signed rank test; *two-tailed p-values<0.05). (C) The effect of Dexa on TCA rate has been examined also by the expression of PDK4, which inhibits pyruvate dehydrogenase and reduces the influx of glycolytic intermediates to TCA. Quantitative PCRs were performed on the panel of WT and A-T lymphoblastoid cell lines with or without Dexa. Fold changes were calculated as the difference between the treated and respective untreated LCL. Values are means and SEM of four independent experiments (Wilcoxon signed rank test, *p-values<0.05).

**FIGURE 7. ENERGETIC STATUS OF WT AND A-T CELLS WITH OR WITHOUT DEXA**

The pools of ATP (A) and NAD (B) have been measured by simultaneous extraction of adenine and pyridine nucleotides followed by HPLC-UV detection. Analyses were performed in A-T cells and in WT cells as control, subjected or not to drug treatment. Values are means and SD of three independent experiments.

**FIGURE 8. EFFECT OF DEXA ON NADK**

The effect of Dexa on NADK was investigated both at mRNA and protein levels. (A) Expression of NADK was assessed by quantitative PCR on WT and A-T LCLs with or without Dexa. Fold changes are expressed as the difference between treated and untreated samples. (B) NADK enzymatic activity has been estimated by spectrophotometric assay on native protein extracts from the same LCLs.

FIGURE 1

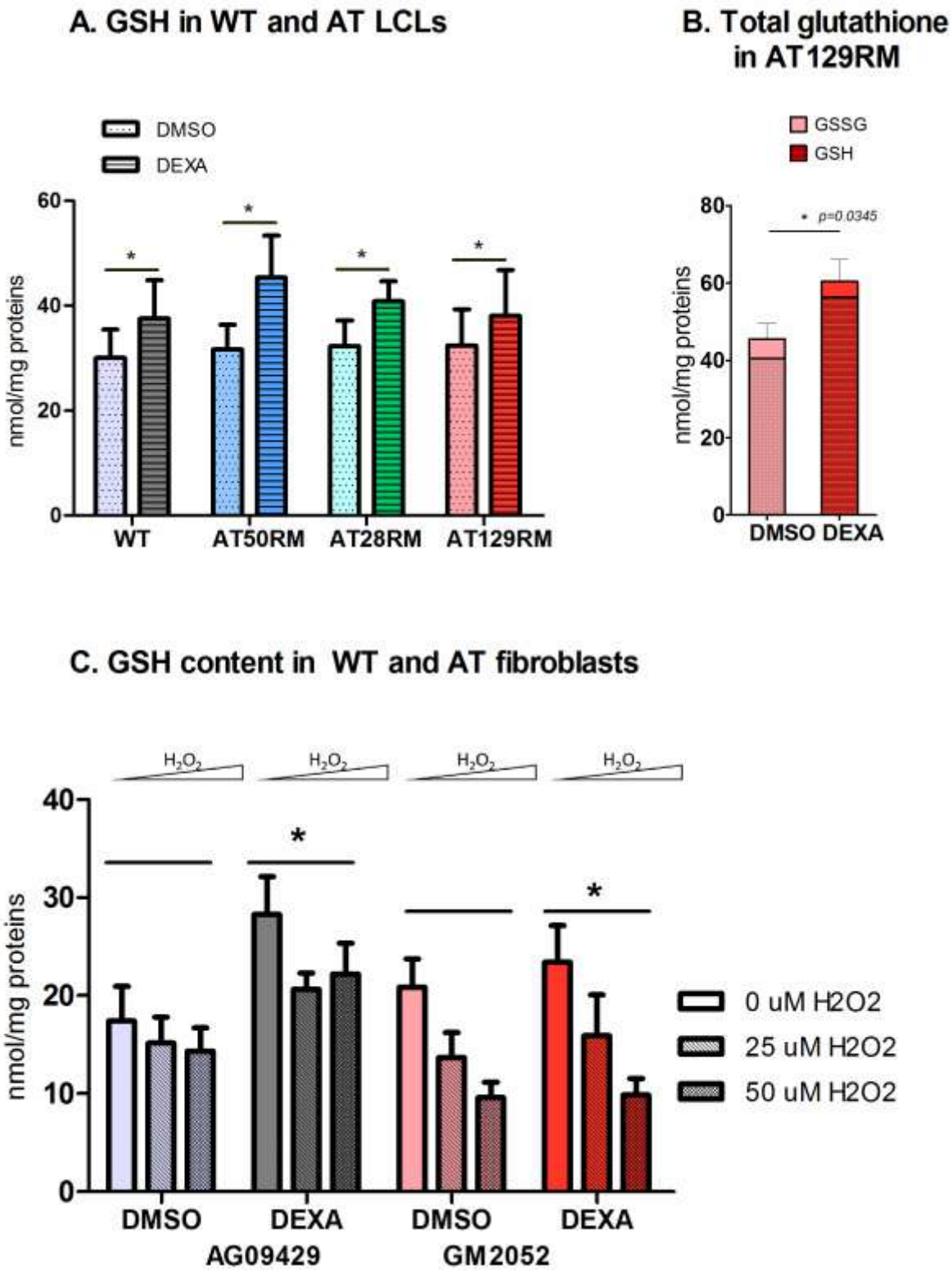
A. GSH in WT and AT LCLs
DMSO
DEXA
nmol/mg proteins
60
40
20
0
*
WT
AT50RM
AT28RM
AT129RM
B. Total glutathione in AT129RM
GSSG
GSH
* p=0.0345
80
60
40
20
0
DMSO DEXA
C. GSH content in WT and AT fibroblasts
H2O2
40
30
20
10
0
DMSO
DEXA
AG09429
GM2052
0 uM H2O2
25 uM H2O2
50 uM H2O2

FIGURE 2

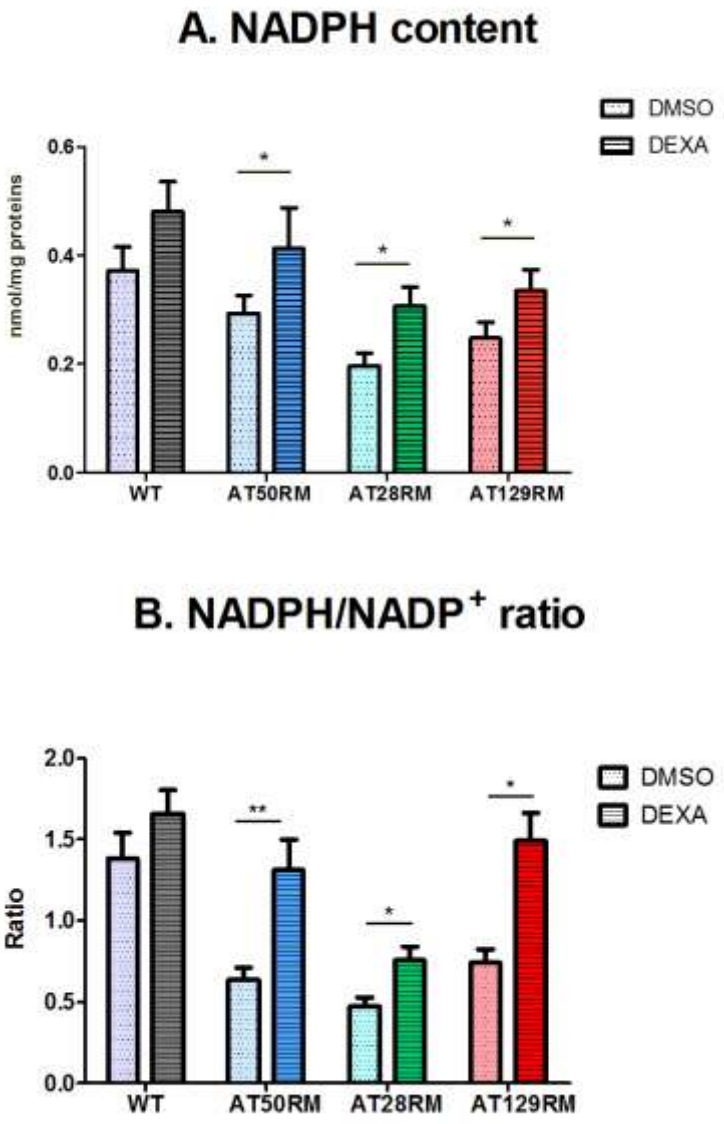
A. NADPH content
DMSO
DEXA
nmol/mg proteins
0.6
0.4
0.2
0.0
*
*
*
WT
AT50RM
AT28RM
AT129RM
B. NADPH/NADP+ ratio
DMSO
DEXA
Ratio
2.0
1.5
1.0
0.5
0.0
**
*
*
WT
AT50RM
AT28RM
AT129RM

FIGURE 3

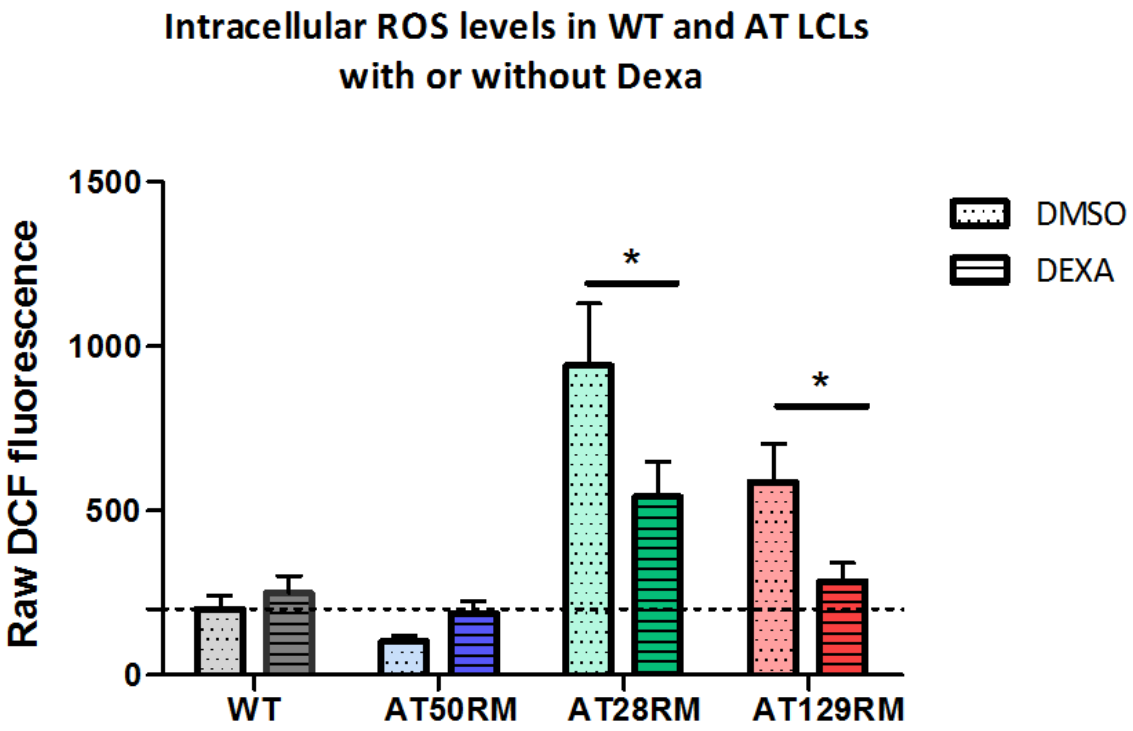
Intracellular ROS levels in WT and AT LCLs
with or without Dexa
Raw DCF fluorescence
1500
1000
500
0
*
*
DMSO
DEXA
WT
AT50RM
AT28RM
AT129RM

FIGURE 4

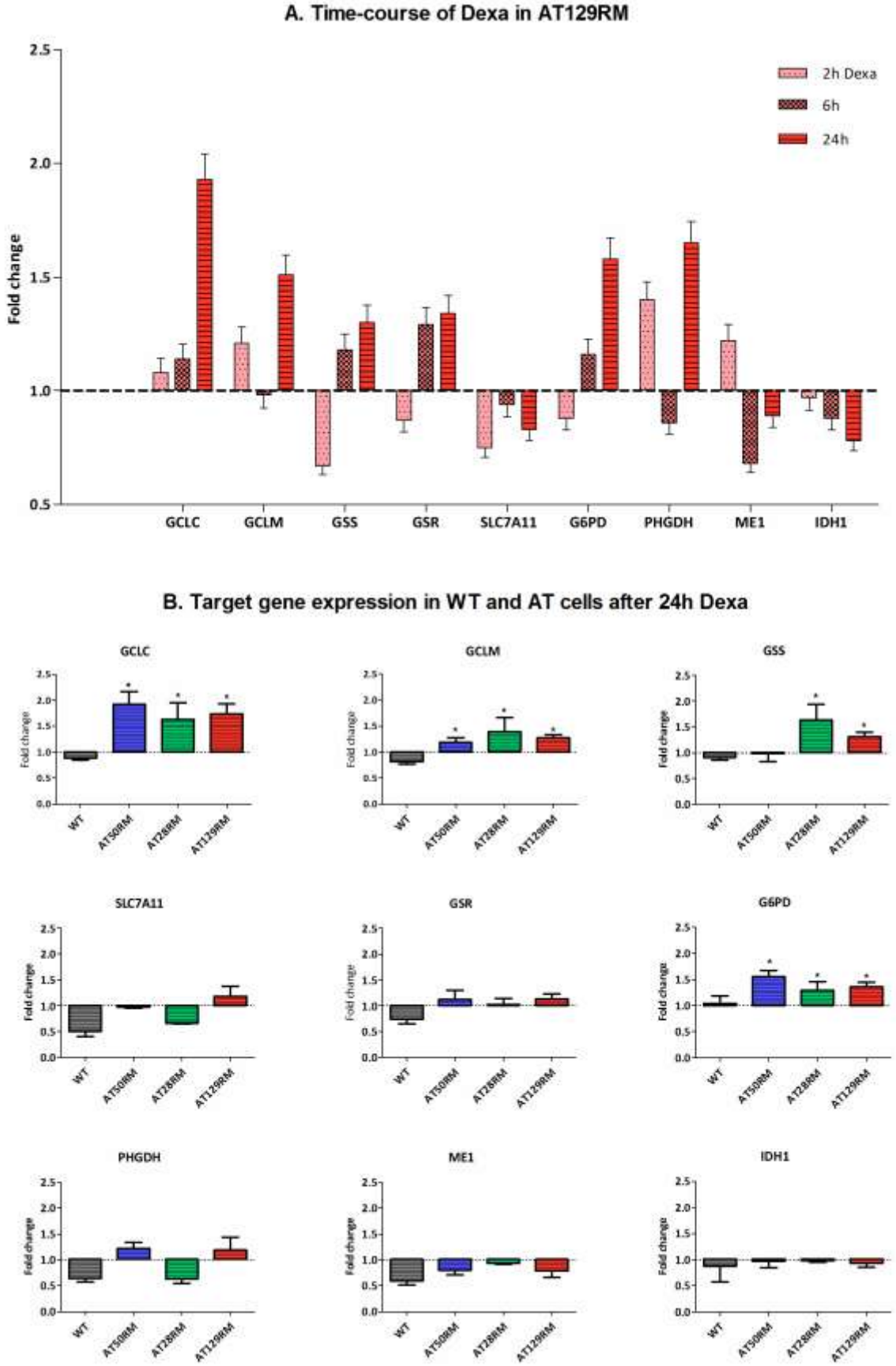
A. Time-course of Dexa in AT129RM
Fold change
2h Dexa
6h
24h
GCLC
GCLM
GSS
GSR
SLC7A11
G6PD
PHGDH
ME1
IDH1
B. Target gene expression in WT and AT cells after 24h Dexa
WT
AT50RM
AT28RM
AT129RM

FIGURE 5

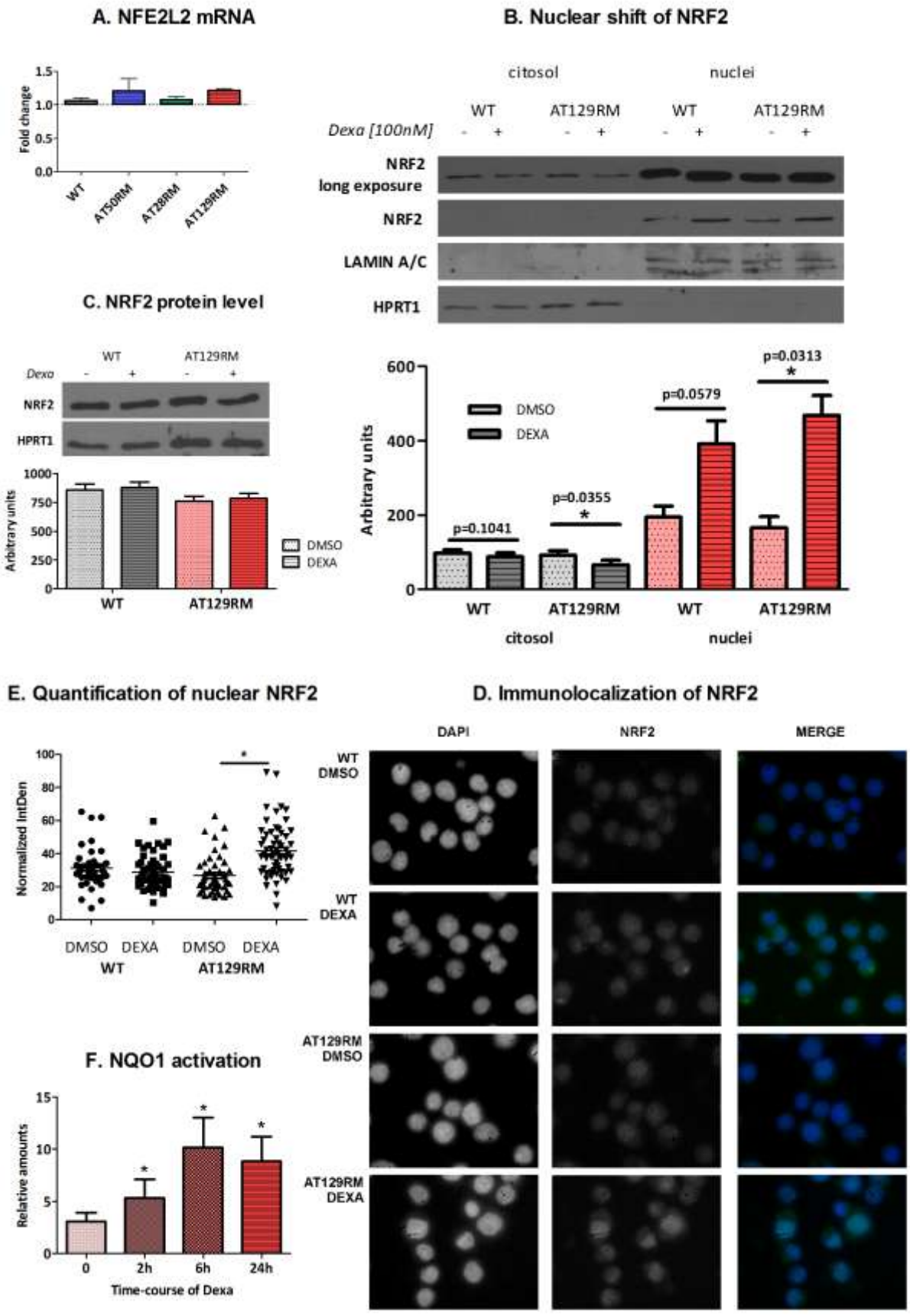
A. NFE2L2 mRNA
Fold change
1.5
1.0
0.5
0.0
WT
AT50RM
AT28RM
AT129RM
B. Nuclear shift of NRF2
citosol
nuclei
WT
AT129RM
WT
AT129RM
Dexa [100nM]
- + - + - + - +
NRF2
long exposure
NRF2
LAMIN A/C
HPRT1
C. NRF2 protein level
WT
AT129RM
Dexa
- + - +
NRF2
HPRT1
Arbitrary units
1000
750
500
250
0
DMSO
DEXA
WT
AT129RM
Arbitrary units
600
400
200
0
DMSO
DEXA
p=0.1041
p=0.0355
*
p=0.0579
p=0.0313
*
WT
AT129RM
WT
AT129RM
citosol
nuclei
E. Quantification of nuclear NRF2
Normalized IntDen
100
80
60
40
20
0
*
DMSO
DEXA
DMSO
DEXA
WT
AT129RM
D. Immunolocalization of NRF2
DAPI
NRF2
MERGE
WT DMSO
WT DEXA
AT129RM DMSO
AT129RM DEXA
F. NQO1 activation
Relative amounts
15
10
5
0
*
*
*
0
2h
6h
24h
Time-course of Dexa

FIGURE 6

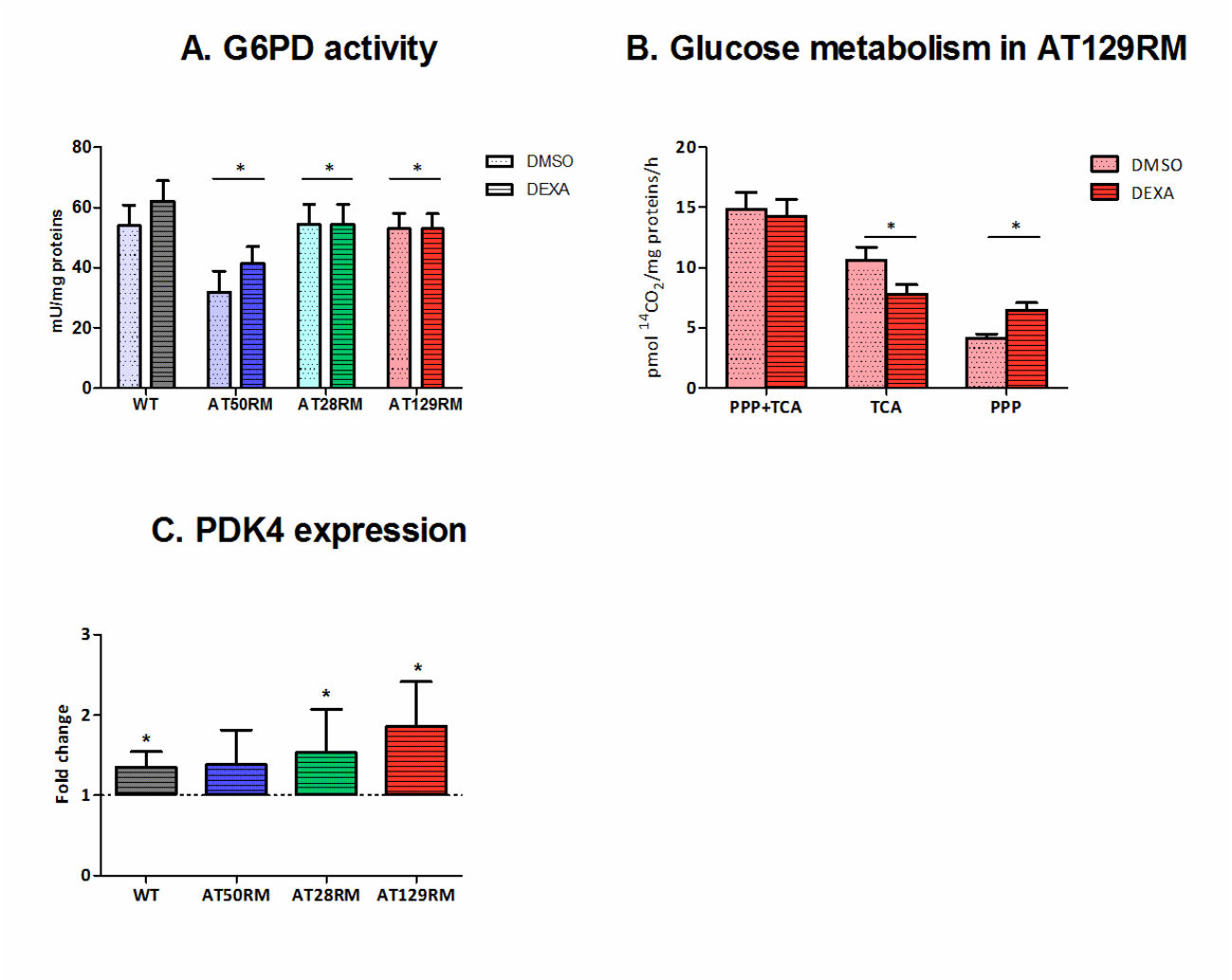
A. G6PD activity
mUI/mg proteins
80
60
40
20
0
*
*
*
DMSO
DEXA
WT
AT50RM
AT28RM
AT129RM
B. Glucose metabolism in AT129RM
pmol $^{14}CO_2$/mg proteins/h
20
15
10
5
0
*
*
DMSO
DEXA
PPP+TCA
TCA
PPP
C. PDK4 expression
Fold change
3
2
1
0
*
*
*
WT
AT50RM
AT28RM
AT129RM

FIGURE 7

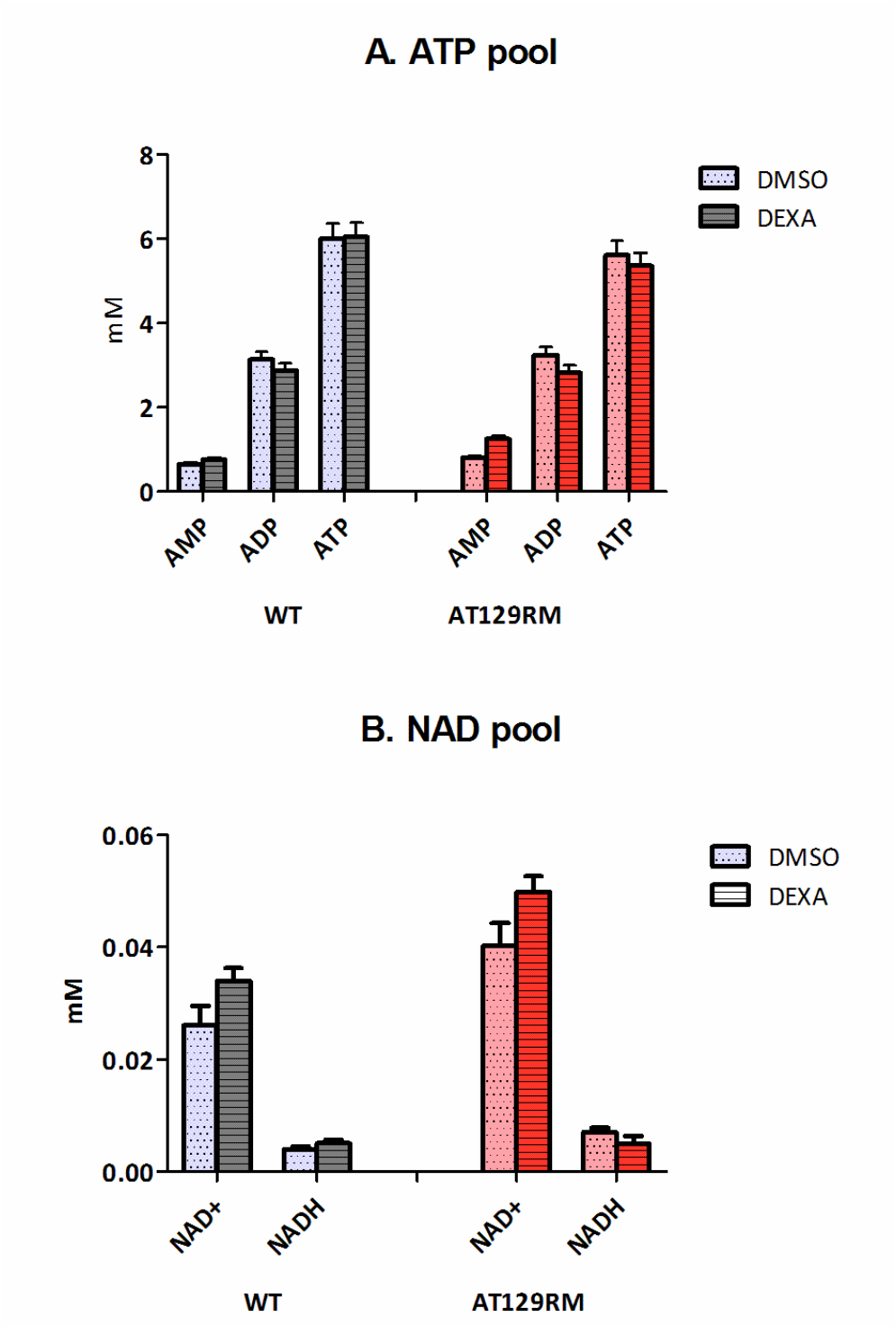
A. ATP pool
8
6
4
2
0
mM
DMSO
DEXA
AMP
ADP
ATP
AMP
ADP
ATP
WT
AT129RM
B. NAD pool
0.06
0.04
0.02
0.00
mM
DMSO
DEXA
NAD+
NADH
NAD+
NADH
WT
AT129RM

FIGURE 8

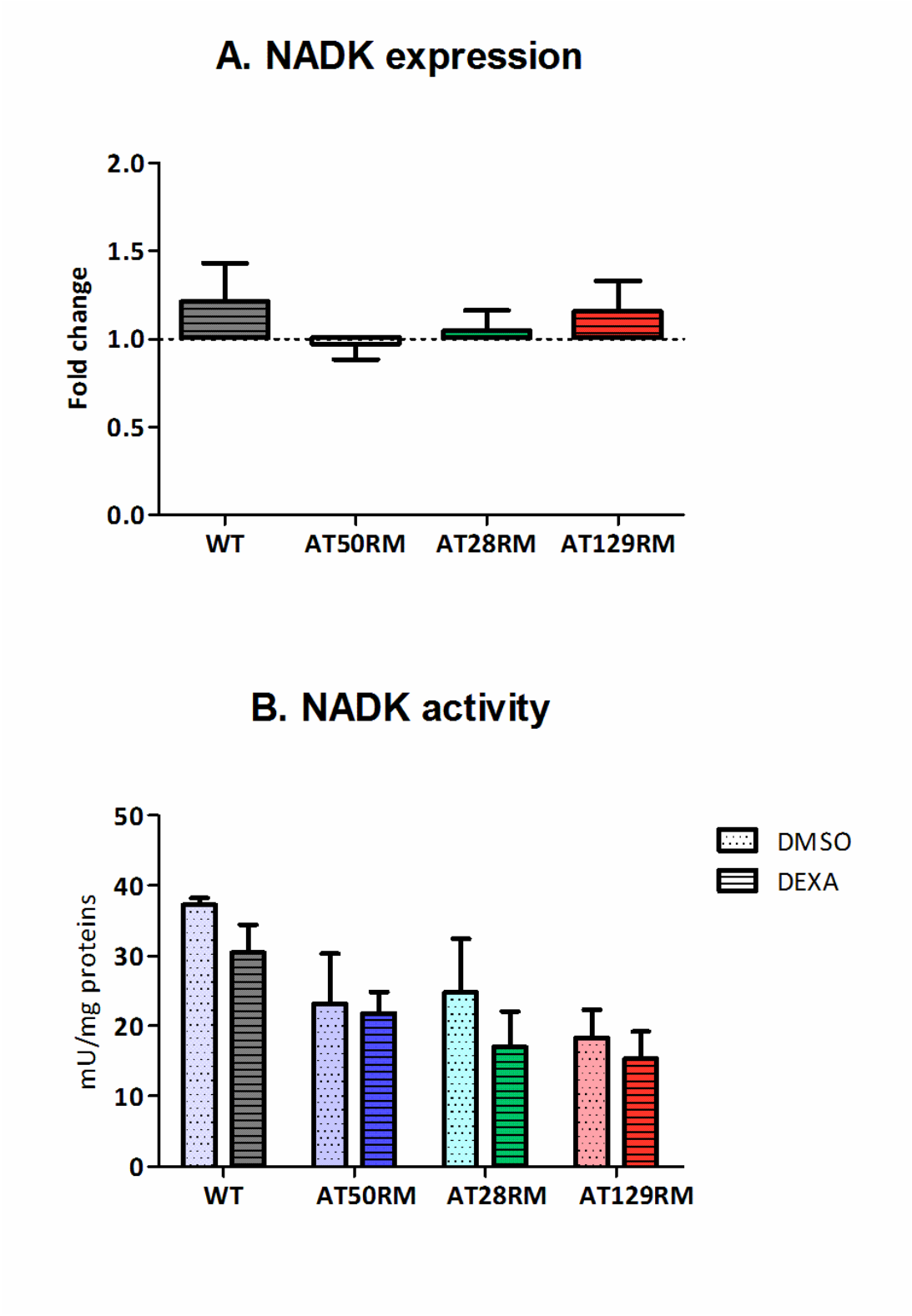
A. NADK expression
Fold change
2.0
1.5
1.0
0.5
0.0
WT
AT50RM
AT28RM
AT129RM
B. NADK activity
mU/mg proteins
50
40
30
20
10
0
DMSO
DEXA
WT
AT50RM
AT28RM
AT129RM